

Observation of the Particle Pinch Velocity Reversal with ITG/TEM

Transition in the Tore Supra Tokamak

X.L. Zou¹, W.L. Zhong², C. Bourdelle¹, S.D. Song², J.F. Artaud¹, T. Aniel¹, X.R. Duan²

¹ *CEA, IRFM, F-13108 Saint-Paul-lez-Durance, France*

² *Southwestern Institute of Physics, P.O. Box 432, Chengdu 610041, China*

Email : xiao-lan.zou@cea.fr

In earlier fully non-inductive current drive experiments with lower hybrid current drive (LHCD) in the Tore Supra tokamak, the existence of an inward turbulent particle pinch is demonstrated in steady-state plasma without toroidal electric field [1]. In tokamak, it has been theoretically shown that the particle pinch driven by the ITG is inward, while that driven by TEM can be outward via the thermal-diffusion term [2]. These features are used in our experiments for the identification of the turbulence modes. High resolution reflectometry measurement [3] of the density profile allows us to investigate in details the particle transport. Density modulation experiments have been performed in the Tore Supra tokamak for determining separately the particle pinch velocity V and particle diffusivity D [4].

The main plasma parameters in the present experiments are the following: the major radius $R=2.4\text{m}$, the minor radius $a=0.72\text{m}$, the plasma current $I_p=1.0\text{MA}$, the magnetic field $B_T=3.3\text{T}$. As shown in Fig.1a, modulation of the Ion Cyclotron Resonance Heating (ICRH) with 2 MW has been used for generating the density perturbation. The electron density profile is measured by two X-mode reflectometers with time resolution of 1ms. The electron temperature is measured by the electron cyclotron emission (ECE) radiometer with time resolution of 1ms. And full ICRH power is modulated at 1Hz with duty cycle of 50%. Fig.1b illustrates the 2D image of the density perturbation during one pulse of ICRH. From this figure it is clear that the density perturbation starts to increase from the Last Closed Flux Surface (LCFS), and then propagates inward. The particle perturbation source can be estimated by $S(r,t)=\partial n_e/\partial t$ when the time difference is short enough, where the particle transport process is negligible. This particle source generated by ICRH is displayed in Fig.1c with 2.2cm of width.

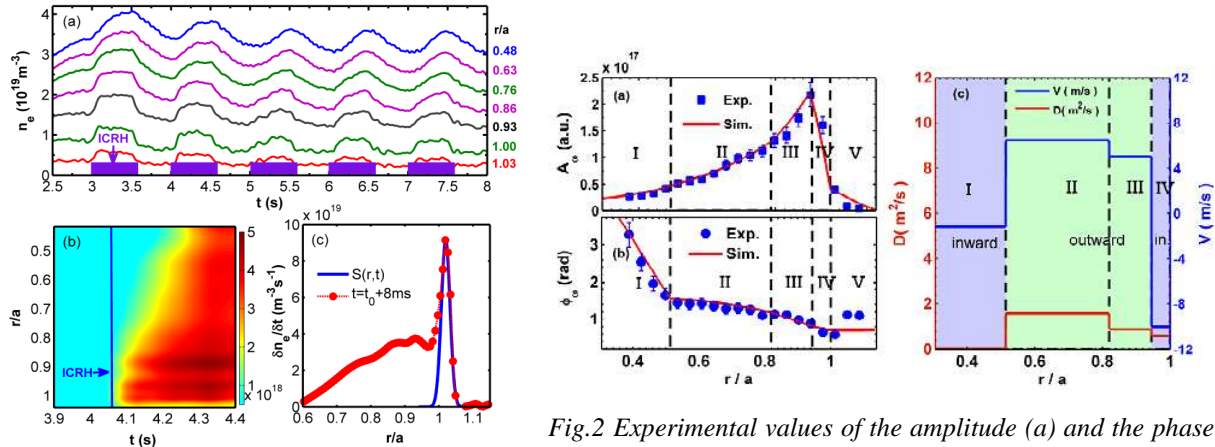


Fig.1 (a) Time evolution of the electron density modulated by ICRH. (b) 2D image of the density perturbation response to the ICRH pulse. (c) The particle source profile deposited by the ICRH pulse.

Fig.2 Experimental values of the amplitude (a) and the phase (b) of the Fourier transform of the density modulated by ICRH. The solid lines represent the simulation results with an analytical transport model using the values of D and V given in (c), where positive V denotes outward pinch and negative V for inward pinch.

The amplitude A_ω and the phase ϕ_ω of the first harmonic of the Fourier transform of the modulated density have been obtained as illustrated in Fig.2a and 2b. To determine D and V , an analytical linear transport model is used to simulate the amplitude and phase of the density perturbation [5]. According to the sharp changes in the amplitude and phase, five zones have been identified as indicated in Fig.2 and Tab.1. From Fig.2b the particle source generated by the ICRH pulse, given by the minimum of the phase, is located at the LCFS, which is consistent with Fig.1c. As shown in Fig.2a and Fig.2b, the best fit (solid line) has been found with the optimized D and V , which are plotted in Fig. 2c, and the values are given in Tab.1. The pinch velocity direction is defined as inward for negative values and outward for positive values.

	Zone I ($0.3 < r/a < 0.52$)	Zone II ($0.52 < r/a < 0.82$)	Zone III ($0.82 < r/a < 0.95$)	Zone IV ($0.95 < r/a < 1.0$)
D (m^2/s)	$D = 0.03 \pm 0.01$	$D = 1.6 \pm 0.1$	$D = 0.9 \pm 0.1$	$D = 0.6 \pm 0.15$
V (m/s)	$V = -1.2 \pm 0.03$	$V = 6.5 \pm 1.5$	$V = 5 \pm 1$	$V = -10 \pm 2$

Tab.1 Values of D and V of Fig.2c in different zones.

As shown in Fig.2c, the pinch velocity reverses at $r/a = 0.52$ between the zones I and II in the plasma core. And at the same position a drastic change in the diffusivity has been observed. The key physical parameters the pinch velocity reversal and diffusivity drastic

change could be the normalized density gradient $R / L_n = -R \nabla n_e / n_e$ and the normalized temperature gradient $R / L_T = -R \nabla T_e / T_e$. The diffusive particle flux is defined as $\Gamma_D = -D \nabla n_e$. The particle flux and the pinch velocity are plotted as function R / L_T in Fig.3. Same threshold in the normalized temperature gradient is clearly observed for the particle flux steep increase and the pinch velocity reversal. This threshold is estimated to be $(R / L_T)_{crit} \approx 8.5$. As shown in Fig.4, similar threshold effect has been observed for the normalized density gradient with $(R / L_n)_{crit} \approx 3.3$. **It should be noted that D and V inferred from modulation experiments are for the transient phase, and are different to that of the steady state.**

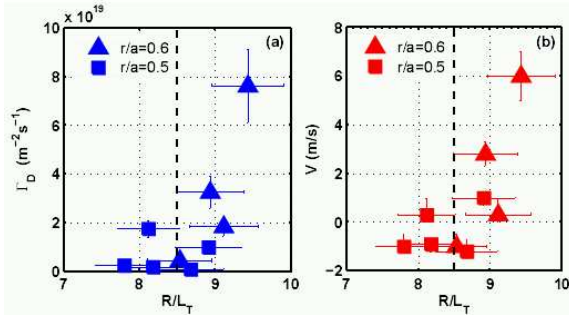


Fig.3 (a) Diffusive particle flux and (b) pinch velocity v.s. R / L_T .

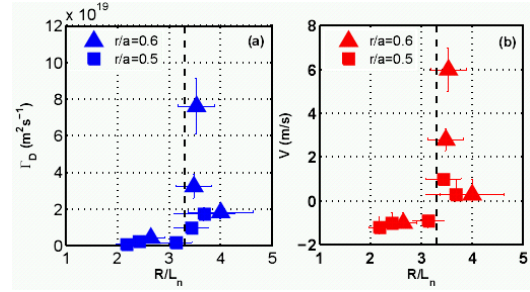


Fig.4 (a) Diffusive particle flux and (b) pinch velocity v.s. R / L_n .

However, some experimental points look very scattered as shown in Fig.3. In fact, the steep increase of the diffusive particle flux and the pinch velocity reversal are determined by both R / L_T and R / L_n . Thus the actual key parameter for the threshold is the combination of these two gradients. The experimental observation can be compared and understood from the theoretical point of view by using a quasilinear gyrokinetic code named QuaLiKiz [6]. Note that only the thresholds can be compared to the simulation, the D and V being the ones of the modulation. The turbulence stability diagram obtained by QuaLiKiz simulations shows that the experimental points with different pinch velocities are separated by the TEM threshold boundary as shown in Fig.5a. The points with inward pinch velocities are located in the ITG unstable region. However, the points with outward pinch velocities are located in the region where both ITG and TEM are unstable. By fitting the threshold boundary with a linear line, the new threshold is given by $\zeta_c = R / L_T + 4(R / L_n) = 22$ for our experimental conditions as shown in Fig.5a. Fig.5b and Fig.5c plot respectively the diffusive flux and pinch velocity as a

function of the new variable $\zeta = R/L_T + 4(R/L_n)$. Both the strong diffusive particle flux increase and the pinch velocity reversal are found when the new variable exceeds the threshold $\zeta_c=22$. The observation of both inward and outward regions in the perturbation experiments shows that the density and temperature gradients in steady state are very close to the boundary of the TEM threshold. Thus it suggests that the density profile is governed by a feedback loop and self-regulating system. When the density gradient is low, only the ITG exists, which induces an additional thermo-diffusion inward particle pinch leading to a density gradient increase. The density gradient increases until it exceeds the threshold triggering the TEM, which leads to an outward thermo-diffusion particle convection. In return this action leads to a density gradient decrease. When the density gradient goes down enough, then the TEM disappears, and only the ITG is present, and so on. This mechanism can explain the density profile stiffness. In steady state and in the core of the plasma, the inward particle convection is balanced by the outward particle diffusive flux. It suggests that the reversal of thermal-diffusion might be the mechanism explaining the experimental observation. It should be noted that the curvature driven pinch [2] remains nearly constant in the present experiments, and is dominated by the thermal-diffusion term.

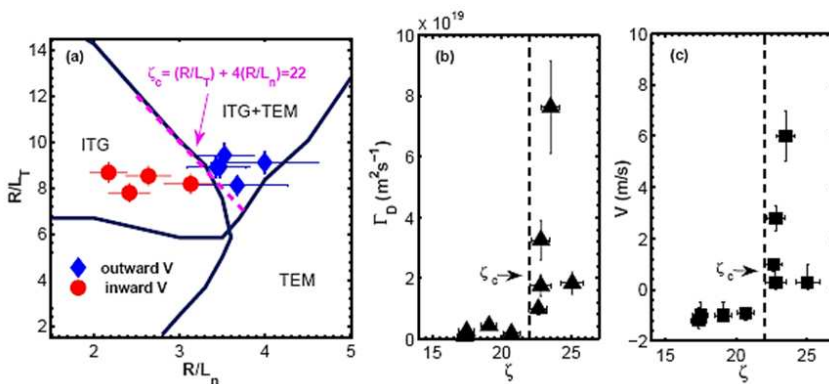


Fig.5 (a) Turbulence stability diagram with QuaLiKiz simulation. The ITG/TEM boundary is fitted with the line of $\zeta_c = R/L_T + 4(R/L_n) = 22$. Diffusive particle flux Γ_D (b) and the pinch velocity V (c) versus ζ .

- [1] G.T. Hoang C. Bourdelle, B. Pégourié *et al.*, Phys. Rev. Lett. **90**, 155002 (2003).
- [2] X. Garbet, L. Garzotti, P. Mantica *et al.*, Phys. Rev. Lett. **91**, 035001(2003)
- [3] F. Clairet, C. Bottereau, J.M. Chareau *et al.*, Plasma Phys. Control. Fusion **43** 429–441 (2001)
- [4] W. W. Xiao, X. L. Zou, X. T. Ding *et al.*, Rev. Sci. Instrum. **81**, 013506 (2010)
- [5] S. P. Eury, E. Harauchamps, X. L. Zou *et al.*, Phys. Plasmas **12**, 102511(2005)
- [6] C. Bourdelle, X. Garbet, F. Imbeaux *et al.*, Phys. Plasmas, **14**, 112501(2007)